



MODULATION OF GRAVITY WAVES BY TIDES AS SEEN IN CRISTA TEMPERATURES

P. Preusse¹, S.D. Eckermann², J. Oberheide¹, M.E. Hagan³, and D. Offermann¹

¹Department of Physics, Wuppertal University (BUGW), Gauss Str. 20, D-42097 Wuppertal, Germany

²E. O. Hulburt Center for Space Research, Naval Research Laboratory, Washington, DC 20375, USA

³High Altitude Observatory, NCAR, 3450 Mitchell Lane, Boulder, CO 80307, USA

ABSTRACT

During shuttle missions STS-66 (November, 1994) and STS-85 (August, 1997) the Cryogenic Infrared Spectrometers and Telescopes for the Atmosphere (CRISTA) acquired temperature data with very high spatial resolution. These are analyzed for gravity waves (GW). The altitude range spans the whole middle atmosphere from the tropopause up to the mesopause. In the upper mesosphere tidal amplitudes exceed values of 10 K. Modulation of GW activity by the tides is observed and analyzed using CRISTA temperatures and tidal predictions of the Global Scale Wave Model (GSWM). The modulation process is identified as a tidally-induced change of the background buoyancy frequency. The findings agree well with the expectations for saturated GW and are the first global scale observations of this process.

© 2001 COSPAR. Published by Elsevier Science Ltd. All rights reserved.

INTRODUCTION

In the mesosphere gravity waves and tides attain high amplitudes. When breaking, they deposit momentum and generate turbulence. Therefore, they are important for mesospheric dynamics in controlling the mean background state of the mesosphere (e.g. McLandress, 1998; Hamilton et al., 1999) as well as for long-term variability such as the Semi Annual Oscillation (SAO, e.g., Burrage et al., 1996). High accuracy lidar measurements frequently exhibit an inversion layer structure (Hauchecorne et al., 1987; Meriwether et al., 1998). This has been investigated by numerical modeling and may be attributed to the interaction of tides and gravity waves (Liu et al., 2000). Numerical modeling of the migrating diurnal tide and comparison to measurements of the Cryogenic Infrared Spectrometers and Telescopes for the Atmosphere (CRISTA) also suggest gravity wave – tidal interactions (Oberheide et al., 2000).

In this paper we investigate the influence of the tides on the mesospheric GW spectrum as observed by the CRISTA instrument. After introducing the CRISTA instrument and giving a short description of data acquisition, temperature retrieval and GW analysis, we briefly overview the tidal activity. This is followed by a discussion of zonal mean gravity wave amplitudes in the background of the tides. The paper concludes with a summary of the findings and gives an outlook to further work.

MEASUREMENT TECHNIQUE AND ANALYSIS

The CRISTA experiment (Offermann et al., 1999) has been successfully flown on shuttle missions STS-66 (November 1994) and STS-85 (August 1997) with an orbit inclined 57° to the equator. In this paper we focus on data from the first flight.

In the upper mesosphere measurements cover latitudes from 52° S to 62° N. Temperatures in the altitude range from 40 to 90 km are retrieved from 15 μm infrared emissions with a precision of better than 1 K (Riese et al., 1999a) for day- and night-time measurements. These data have sufficient quality to be investigated for GW.

We isolate the GWs from the background atmosphere thermal structure and from planetary-scale waves as follows. Since the most prominent Rossby waves and Kelvin waves are thought to have low zonal wavenumbers (1–4), we employ a 0–6 zonal wavenumber Kalman filter, which accounts for most planetary waves

Report Documentation Page

Form Approved
OMB No. 0704-0188

Public reporting burden for the collection of information is estimated to average 1 hour per response, including the time for reviewing instructions, searching existing data sources, gathering and maintaining the data needed, and completing and reviewing the collection of information. Send comments regarding this burden estimate or any other aspect of this collection of information, including suggestions for reducing this burden, to Washington Headquarters Services, Directorate for Information Operations and Reports, 1215 Jefferson Davis Highway, Suite 1204, Arlington VA 22202-4302. Respondents should be aware that notwithstanding any other provision of law, no person shall be subject to a penalty for failing to comply with a collection of information if it does not display a currently valid OMB control number.

1. REPORT DATE 2001		2. REPORT TYPE		3. DATES COVERED 00-00-2001 to 00-00-2001	
4. TITLE AND SUBTITLE Modulation of Gravity Waves by Tides as Seen in Crista Temperatures				5a. CONTRACT NUMBER	
				5b. GRANT NUMBER	
				5c. PROGRAM ELEMENT NUMBER	
6. AUTHOR(S)				5d. PROJECT NUMBER	
				5e. TASK NUMBER	
				5f. WORK UNIT NUMBER	
7. PERFORMING ORGANIZATION NAME(S) AND ADDRESS(ES) Naval Research Laboratory, E.O. Hulburt Center for Space Research, Washington, DC, 20375				8. PERFORMING ORGANIZATION REPORT NUMBER	
9. SPONSORING/MONITORING AGENCY NAME(S) AND ADDRESS(ES)				10. SPONSOR/MONITOR'S ACRONYM(S)	
				11. SPONSOR/MONITOR'S REPORT NUMBER(S)	
12. DISTRIBUTION/AVAILABILITY STATEMENT Approved for public release; distribution unlimited					
13. SUPPLEMENTARY NOTES					
14. ABSTRACT see report					
15. SUBJECT TERMS					
16. SECURITY CLASSIFICATION OF:			17. LIMITATION OF ABSTRACT	18. NUMBER OF PAGES	19a. NAME OF RESPONSIBLE PERSON
a. REPORT unclassified	b. ABSTRACT unclassified	c. THIS PAGE unclassified			

(compare Fetzer and Gille, 1994; Eckermann and Preusse, 1999, for applications of the Kalman filter see Offermann et al., 1999 and Riese et al., 1999b). However, a Kalman filter cannot resolve any waves with periods shorter than a few days and hence cannot resolve the diurnal and semidiurnal tide. This problem can be avoided by separating the data from the ascending (asc.) and the descending (dsc.) orbital nodes. If we consider only asc. orbital nodes, each latitude is measured at a nearly fixed local time and therefore the migrating tide is observed at a fixed phase independent of longitude. On Nov 5, for example, the equatorial data were measured close to 9 am on the asc. and close to 9 pm on the dsc. nodes. Towards higher latitudes the time difference decreases and vanishes at the highest (turnaround) latitudes sampled (Ward et al., 1999). For instance, in the subtropics (30° latitude) the time difference is ~ 9 hours. Measurements at the same latitude are taken at the same local time for asc./dsc. nodes, respectively. This results in a "phase-locking" of the tides, which is discussed in detail by Ward et al. (1999). In particular, this means that all components of the migrating tides alias to the the daily zonal mean of the asc. and dsc. nodes, respectively, and that the non-migrating tides alias to the quasi-stationary integer zonal wavenumbers. A non-migrating tide in the CRISTA data with a vertical wavelength of 26 km sampled as a wave 1 is discussed by Ward et al. (1999). The slowly varying offset caused by the migrating tides (diurnal as well as semidiurnal) and the planetary wave structures caused by the non-migrating tides are captured by the Kalman filter, although the Kalman filter is not able to resolve these modes explicitly. Estimating the background atmosphere and detrending the data separately for asc. and dsc. orbital nodes allows us to remove the tides as well as the planetary waves. The resulting temperature residuals contain gravity wave fluctuations (Fetzer and Gille, 1994; Eckermann and Preusse, 1999).

To characterize these waves, individual vertical profiles were analyzed using the Maximum Entropy Method (MEM) and harmonic analysis (HA). The MEM spectrum was calculated using the complete height profile. The MEM peaks were used to constrain harmonic fits to the profile within a 13 km altitude window that was moved upwards in 1.5 km increments to span the full height range. This MEM/HA analysis provides height profiles of the amplitudes, phases and vertical wavelengths of the two largest oscillations in any given profile, and allows these values to vary with height. The analysis method is described in detail by Preusse et al. (2001), who compare the results so obtained to standard deviations and spectral densities from the Fourier Transform (FT).

OBSERVED TIDAL AND GRAVITY WAVE ACTIVITY

To study the influence of the tides on GWs, it is essential to verify that there are no spurious tidal contributions to the observed GW activity due to the analysis method. This question arises because tidal amplitudes grow in the upper mesosphere up to more than 10 K. This is illustrated in Figure 1, which shows zonal mean profiles measured at the equator for the asc. and dsc. orbit. There are large wave-like differences between the two profiles, which take values up to nearly 20 K at 75 km altitude. Ward et al. (1999) and Oberheide et al. (2000) have shown that these differences are associated with the migrating diurnal tide. Oberheide et al. (2000) have compared the tide as observed in the CRISTA data with results obtained from the Global Scale Wave Model (GSWM, see, e.g., Hagan et al., 1995) and found excellent agreement. The observed vertical wavelength is about 20 km.

Therefore we choose the wavelength range around 20 km to verify that the analysis properly distinguishes between GWs and tides. Figure 2 compares zonal mean amplitudes of GWs having vertical wavelengths in the range from 17 km to 25 km with the tidal amplitudes from the GSWM. Panel (a) shows a GW analysis for which the detrending is based on one zonal mean calculated from asc. and dsc. nodes together. In the tropics this zonal mean contains no contribution from the diurnal and semidiurnal migrating tide because of the 12-hour time difference between asc. and dsc. nodes. Temperature residuals from the zonal mean are therefore expected to contain tidal and planetary waves as well as GWs. The amplitudes shown in panel (a) are therefore much larger than in panel (b), which provides GW amplitudes inferred by separately detrending the asc. and dsc. nodes employing the Kalman filter. However, the amplitudes in Figure 2a contain the salient features of the expected tidal amplitudes predicted by the GSWM which are given in panel (c). Particularly at equatorial latitudes, where the tides dominate, good agreement is found. The high values at northern mid and high latitudes found in panel (a) probably indicate planetary wave activity. The further discussion is based on waves with vertical wavelength between 6.0 km and 9.0 km. Since this

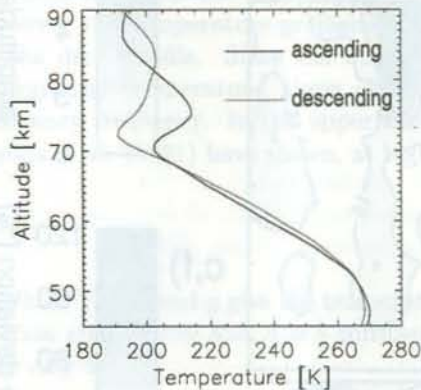


Fig. 1. Zonal mean profiles at the equator (10 S to 10 N) from ascending (solid line) and descending (dashed line) orbits. Separated by a local time lag of 12 hours, the difference between the two profiles can be attributed to the migrating diurnal tide (e.g., Ward et al., 1999).

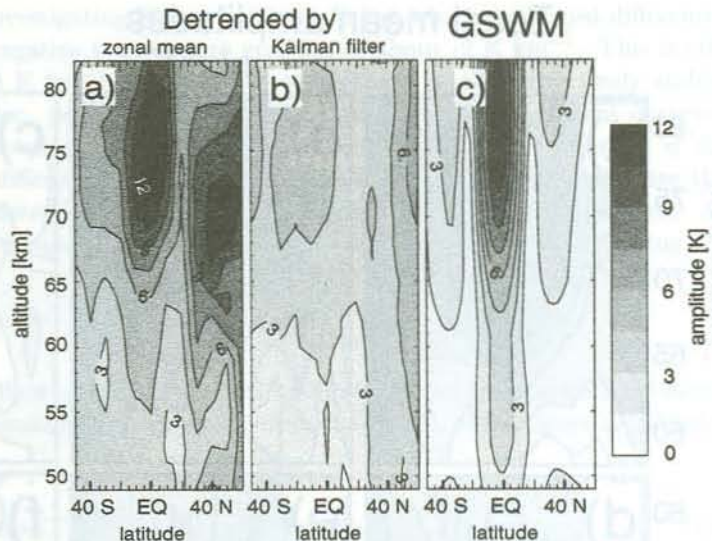


Fig. 2. Comparison of GW amplitude with tidal amplitudes of the GSWM. Panels a) and b) show zonal mean amplitudes of GW with vertical wavelengths in the range from 17 km to 25 km. For panel a) data have been detrended with a zonal mean containing ascending as well as descending orbits. Planetary wave and tidal contributions are visible and the equatorial amplitudes compare well with those predicted by the GSWM shown in panel c). Panel b) shows the same analysis, but now the temperatures have been detrended by a 0-6 zonal wavenumber Kalman filter, separately for ascending and descending orbits. The tidal contributions vanish in panel b).

is a completely different wavelength range, we expect that the spectral analysis technique (MEM/HA, see above) would highly suppress any influences of the much longer tidal waves. The results presented in Figure 2 support the inference that separate GW and tidal signals discussed below are real and not induced by the analysis technique.

Zonal means of GW amplitudes for vertical wavelengths ranging from 6.0 km to 9.0 km measured on November 5, 1994 are given in Figure 3. Values from the asc. nodes only are shown in panel (a), values from the dsc. nodes are given in panel (b). The two panels exhibit considerable differences especially at the equator. The values measured on the asc. nodes show a peak at 70 km altitude and decrease strongly at higher altitudes. The values on the dsc. nodes increase nearly monotonically to the upper boundary of the analysis. These differences are quantified in panel (c), which gives the percentile deviation of the values from the dsc. nodes (b) from those on the asc. nodes (a). Deviations of more than 100 % are seen.

Since both means are inferred from a complete coverage of all longitudes the only difference¹ is the local time of the measurements of 9 am and 9 pm for the asc. and dsc. nodes, respectively. The difference in local time implies a difference in the phase of the tides and we therefore can assume that the observed large deviations are related to the tides. Commonly the modulation of GW is discussed in terms of wind modulation (e.g. Alexander, 1998, Eckermann and Preusse, 1999, McLandress et al., 2000). We therefore examine the migrating tidal wind field as calculated by the GSWM given in Figure 4. Panels (a) and (b) show the zonal and meridional wind amplitude of the migrating diurnal tide. The velocity amplitudes are very small at the equator, thus we conclude that the migrating tides influence the equatorial GWs in a different manner.

¹The two measurement sets differ also in the viewing geometry (c.f. Figure 2 of Riese et al., 1999a). This was shown to have large influences in analyses of saturated radiances as measured by the Microwave Limb Sounder (MLS) by Wu and Waters (1997) and McLandress et al. (2000) and utilized to achieve information about the propagation direction of the waves. Since CRISTA infers temperatures from optically thin emissions these effects do not influence the current analysis (c.f. Preusse et al., 2001).

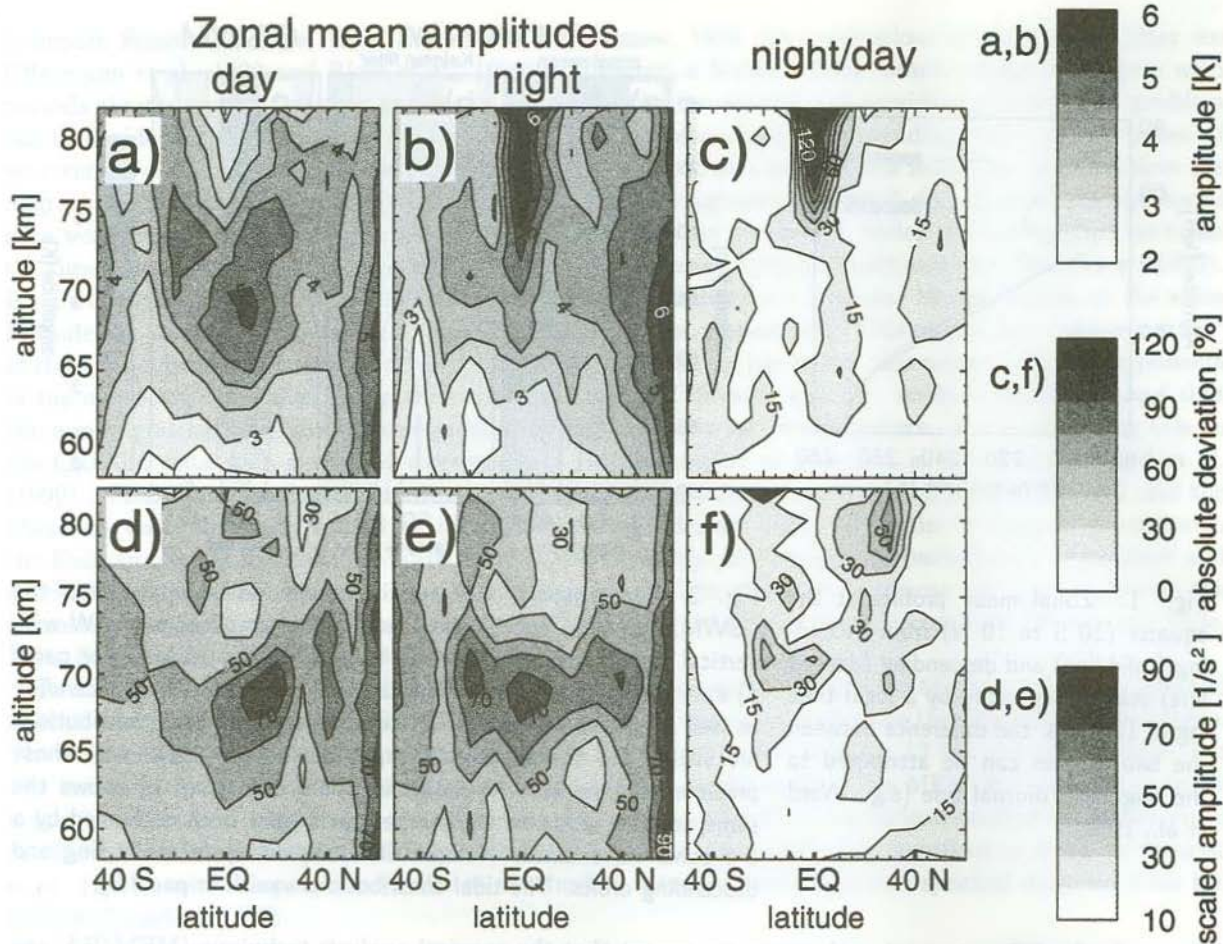


Fig. 3. Comparisons of asc. and dsc. values of zonal mean GW amplitudes for the vertical wavelength range 6–9 km. Zonal means of GW amplitudes for asc. and dsc. are given in panels (a) and (b) respectively. Panel (c) shows the absolute value of the percentile deviation of the dsc. GW amplitudes from the asc. values. The large differences disappear when rescaling the amplitudes by a factor $1/(TN^2)$, which leads accordingly to GW theory to a constant. Panel (d) and (e) give the rescaled asc. and dsc. values respectively and panel (f) again the absolute percentile deviations of the dsc. from the asc. values. For details, see text.

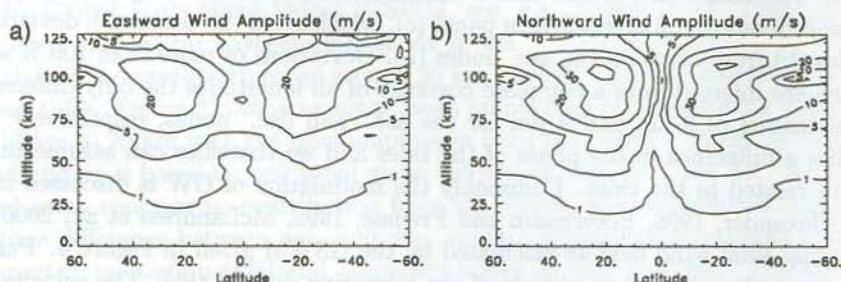


Fig. 4. Wind amplitudes of the migrating diurnal tide as calculated by the GSWM (October values). Panel (a) gives the zonal, panel (b) the meridional wind component. The amplitudes vanish at the equator and reach maximum values in the subtropics around 20° north and south. Contour labels are in $m s^{-1}$.

This mechanism becomes evident by re-investigating Figure 1. Above 70 km, where the largest differences appear, the asc. profile exhibits a strong negative temperature gradient of about -2 K km^{-1} . This is still far from the adiabatic lapse rate $\Gamma \simeq -10 \text{ K km}^{-1}$ and thus the atmosphere is still convectively stable. However the temperature gradient in the asc. profile is much smaller than the positive gradient observed in the dsc. profile. Since the buoyancy frequency N is given by $N^2 = g/T(\partial_z T - \Gamma)$, where T is the background temperature, these observed differences in temperature gradient will strongly influence the buoyancy frequency. In the upper mesosphere GWs at wavelengths shorter than 9 km are saturated. As Tsuda et al. (1991) have shown, at high wavenumbers the temperature power spectra follow the scaling law

$$F_T'(m) = \left(\frac{TN^2}{g}\right)^2 \frac{A}{m^3} \quad (1)$$

where T' , m and g give the temperature fluctuation, the vertical wavenumber and the gravitational acceleration respectively and A is a constant. Considering a given wavelength interval, temperature amplitudes will vary as

$$T'^2 = \text{const} * (T^2 N^4) \Rightarrow \frac{T'}{TN^2} = \text{const} \quad (2)$$

When calculating $T'/(TN^2)$ from the CRISTA data, the differences between asc. and dsc. values should vanish. This has been tested in Figure 3, panels (d), (e) and (f). The background temperature T and buoyancy frequency N are evaluated from the background atmosphere used for the detrending. The values have been calculated for the individual profiles and separately for the two local times. Corresponding to Figure 3, panels (a), (b) and (c), panels (d), (e) and (f) give asc. values, dsc. values and deviations respectively. As can be seen from panel (f) the strong asc.-dsc. differences at the equator are compensated by the variations of the buoyancy frequency. Differences now appear in the subtropics where the wind amplitudes of the tides are strong, thus possible subtropical tidal wind modulations are more visible in the scaled amplitudes.

Tsuda et al. (1991) also discussed whether the factor A in Equation 1 depends on the spectral distribution of the wave frequency and on the strength of wave dissipation. In particular, A increases with increasing dissipation. Since the altitude range considered is small and a substantial change of the frequency distribution is therefore unlikely, the maximum observed in Figures 3d and 3e at 70 km altitude might indicate enhanced wave breaking. It is interesting that this feature nearly coincides with a temperature inversion visible in Figure 1 just above 70 km. However, the question whether wave breaking is the reason for the enhanced values in Figures 3d and 3e should be investigated in more detail with the help of future numerical modeling efforts.

Has this apparent GW interaction with tidal temperature variations in the equatorial mesosphere been noted before? Miyahara and Forbes (1994) provided indirect evidence of it by noting that large diurnal temperature variations at the equator caused their linear gravity wave parameterization schemes to fail there, due to WKB violations due to small tidally-produced background N values. They also discussed a general circulation model study that seemed to show that these GW interactions enhanced the production of convective instabilities. The role of GW-tidal interactions in producing temperature inversions and convective overturning in the mesosphere generally is a topic of current interest (e.g. Liu et al., 2000).

SUMMARY AND CONCLUSIONS

Zonal means of gravity wave amplitudes have been investigated in the upper mesosphere and strong variations depending on local time of the measurements have been found around the equator. These can be attributed to the strong thermal migrating diurnal tide observed in this region. The tide modulates the background buoyancy frequency and modulates thereby the observed GW activity. The findings in the observations are in good agreement with the theory of saturated GWs as presented by Tsuda et al. (1991) at high wavenumbers (corresponding to a vertical wavelength range of 6-9 km). This process is substantially different from the modulation of GW flux by the wind speed. An impact of the GW modulation on the deposition of GW momentum at higher altitudes can be expected and the process should therefore influence the mesospheric tidal structure as well as the background state of the upper mesosphere.

ACKNOWLEDGMENT

The CRISTA experiment is funded by the Bundesministerium fuer Bildung und Forschung (BMBF, Berlin) through Deutsches Zentrum fuer Luft- und Raumfahrt (DLR, Bonn). SDE's research was supported by NASA's UARS Guest Investigator Program (NAS5-98045) and the Office of Space Science.

REFERENCES

- Alexander, M. J., Interpretations of Observed Climatological Patterns in Stratospheric Gravity Wave Variance, *J. Geophys. Res.*, **103**, 8627-8640, 1998.
- Burrage, M. D., R. A. Vincent, H. G. Mayr, W. R. Skinner, N. F. Arnold and P. B. Hays, Long-term Variability in the Equatorial Middle Atmosphere Zonal Wind, *J. Geophys. Res.*, **101**, 12,847-12,854, 1996.
- Eckermann, S. D. and P. Preusse, Global Measurements of Stratospheric Mountain Waves from Space *Science*, **286**, 1534-1537, 1999.
- Fetzer, E. J., and J. C. Gille, Gravity Wave Variance in LIMS Temperatures. Part I: Variability and Comparison with Background Winds, *J. Atmos. Sci.*, **51**, 2461-2483, 1994.
- Hagan, M. E., J. M. Forbes, and F. Vial, On Modeling Migrating Solar Tides, *Geophys. Res. Lett.*, **22**, 893-896, 1995.
- Hamilton, K., R.J. Wilson and R.S. Hemler, Middle Atmosphere Simulated with High Vertical and Horizontal Resolution Versions of a GCM: Improvements in the Cold Pole Bias and Generation of a QBO-like Oscillation in the Tropics *J. Atmos. Sci.*, **56**, 3829-3846, 1999.
- Hauchecorne, A., M. L. Chanin, and R. Wilson, Mesospheric Temperature Inversion and Gravity Wave Breaking, *Geophys. Res. Lett.*, **14**, 933-936, 1987.
- Liu, H.-L., M. E. Hagan, and R. G. Roble, Local Mean State Changes due to Gravity Wave Breaking Modulated by Diurnal Tide *J. Geophys. Res.*, **105**, 12,381-12,396, 2000.
- McLandress, C., On the Importance of Gravity Waves in the Middle Atmosphere and Their Parameterization in General Circulation Models, *J. Atmos. and Solar-Terr. Phys.*, **60**, 1357-1383, 1998.
- McLandress, C., M. J. Alexander and D. L. Wu, Microwave Limb Sounder Observations of Gravity Waves in the Stratosphere: a Climatology and Interpretation, *J. Geophys. Res.*, **105**, 11,947-11,967, 2000.
- Meriwether, J. W., X. Gao, V. B. Wickwar, T. Wilkerson, K. Beissner, S. Collins, M. E. Hagan, Observed Coupling of the Mesosphere Inversion Layer to the Thermal Tidal Structure, *Geophys. Res. Lett.*, **25**, 1479-1482, 1998.
- Miyahara, S., and J. M. Forbes, Interaction Between Diurnal Tides and Gravity Waves in the Lower Thermosphere, *J. Atmos. Terr. Phys.*, **56**, 1365-1373, 1994.
- Oberheide, J., M. E. Hagan, W. E. Ward, M. Riese and D. Offermann, Modeling the Diurnal Tide for the CRISTA 1 Time Period, *J. Geophys. Res.*, **105**, 24,917-24,929, 2000.
- Offermann, D., K. U. Grossmann, P. Barthol, P. Knieling, M. Riese, and R. Trant, The Cryogenic Infrared Spectrometers and Telescopes for the Atmosphere (CRISTA) Experiment and Middle Atmosphere Variability, *J. Geophys. Res.*, **104**, 16,311-16,325, 1999.
- Preusse, P., A. Doernbrack, S.D. Eckermann, K.-A. Tan, M. Riese, B. Schaeler, D. Broatman, J. Bacmeister and D. Offermann, Space Based Measurements of Stratospheric Mountain Waves by CRISTA, 1., Sensitivity, Method and a Case Study, *J. Geophys. Res.*, to be submitted, 2001.
- Riese, M., R. Spang, P. Preusse, M. Ern, M. Jarisch, D. Offermann, and K. U. Grossmann, CRISTA Data Processing and Atmospheric Temperature and Trace Gas Retrieval, *J. Geophys. Res.*, **104**, 16,349-16,367, 1999a.
- Riese, M., X. Tie, G. Brasseur and D. Offermann, Three Dimensional Simulations of Stratospheric Trace Gas Distributions Measured by CRISTA, *J. Geophys. Res.*, **104**, 16,419-16,435, 1999b.
- Tsuda, T., T. E. VanZandt, M. Mizumoto, S. Kato and S. Fukao, Spectral Analysis of Temperature and Brunt-Vaisala Frequency Fluctuations Observed by Radiosondes, *J. Geophys. Res.*, **96**, 17,265-17,278, 1991.
- Ward, W.E., J. Oberheide, M. Riese, P. Preusse, and D. Offermann, Tidal Signatures in Temperature Data from the CRISTA I Mission, *J. Geophys. Res.*, **104**, 16,391-16,403, 1999.
- Wu, D. L. and J. W. Waters, Observations of Gravity Waves with the UARS Microwave Limb Sounder, in *Gravity Wave Processes and Their Parameterization in Global Climate Models*, edited by K. Hamilton, Springer Verlag, New York, 1997.